Intelligent approach to Force/Position Control of Ultrasound-Guided Breast Biopsy Robotic System

Mohammad Afif Ayob[1], Wan Nurshazwani Wan Zakaria[1], Jamaludin Jalani[2], Mohd Razali Md Tomari[1], Anis Azwani Muhd Suberi[1], and Tee Kian Sek[1], and Nik Farhan Nik Fuad[3]
[1]*ADvanced Mechatronics Research Group (ADMIRE), Faculty of Electrical and Electronic Engineering, Universiti Tun Hussein Onn Malaysia, 86400 Parit Raja, Batu Pahat, Malaysia.*
[2]*Department of Electrical Engineering Technology, Faculty of Engineering Technology, Universiti Tun Hussein Onn Malaysia, 86400 Parit Raja, Batu Pahat, Malaysia.*
[3]*UKM Medical Centre, Jalan Yaacob Latif, Bandar Tun Razak, Cheras Kuala Lumpur,56000,Malaysia*
shazwani@uthm.edu.my

***Abstract*—Large deformations occur inside the breast whenever the biopsy needle is inserted during conventional ultrasound-guided breast biopsy procedure. Inconsistent force from manual handling of the ultrasound transducer makes maintaining the suspected lump in the ultrasound-imaging region challenging and further position the patient at discomfort. Hence, this research presents the development of force controller for an ultrasound-guided breast biopsy (UGBB) robotic system in the aims to alleviate said issues by maintaining low contact force on the breast. A variant of force controllers has been studied; proportional (P), proportional and integral (PI), PID, PI-Fuzzy, Fuzzy-PID (F-PID), and Fuzzy-PID using Lookup Table (F-LUT) controllers. Effect of external disturbance such as subject respiration is considered to see the reliability of each developed force/position control system. Based on the simulation results, F-PID force controller shows promising outcome with a marginal error of 0.33% during the disturbance period and no error when the disturbance is absent.**

***Index Terms*—Breast biopsy; Force/Position control; Robotic system; Ultrasound-Guided.**

I. INTRODUCTION

Needle biopsy and open excisional biopsy are two notable approaches for breast biopsy [1]. Previous research proves that the overall accuracy of this extremely safe assessment is 99.6% and the error only contributes to 1.7 per 1000 women discharged over a 3-year period [2]. Image-guided needle biopsy is more appealing because it is less traumatic, produces little or no scar [3]–[5], allows quicker recovery, and substantially low cost than open surgical biopsy [6]. However, accuracy in such procedure differs from one surgeon to another [7]. A precise localization gradually become further challenging for a deeper and smaller size breast lesion even with extensive training [8]. Moreover, due to the dynamic structures of the breast tissue, large deformations occur inside the breast whenever the biopsy needle is inserted [9]. These deformations along with the consequences of inconsistent exerted force from the ultrasound transducer to the breast makes the suspected tumor to move away from its original position and subsequently disappear from the ultrasound-imaging region. Therefore, a robust hybrid force and position control of an UGBB robotic system is proposed to compensate for tissue deformation, maintain contact force and simultaneously track the suspected tumor.

The control architecture of the proposed UGBB robotic system is illustrated in Fig. 1. The structure is developed based on the external force control scheme which has been proved to be the best solution on safety constraints, simplicity and high rejection rates for disturbances in the actuation system [10], it does not cause the downside of kinematic instability [11], and guarantees that all directions in space are always fully controlled [12]. In this control architecture, the actual MELFA CR1 robot controller is simulated by the position control law in MATLAB Simulink environment. At its core, the position control law consists of forward and inverse kinematics algorithms. Looking at the figure, desired Cartesian position, X_d of the robot end-effector is translated to joint angle for each arms of the robot by the inverse kinematics before being fed to its SimMechanics model. The actual joint angles from the model are then translated using forward kinematics to get the actual Cartesian position of the robot end-effector, X_a. The actual and desired positions are then compared to correct the robot position, X_R. Both position and force controls are simultaneously realized with the position of the robot, X_R being controlled by varying the desired contact force, F_d.

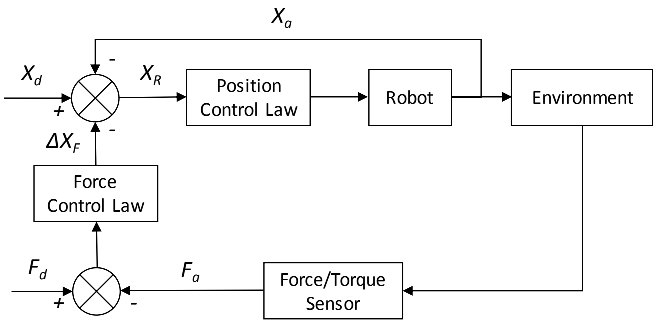

Figure 1: Control Architecture of Proposed UGBB Robotic System

The environment in this architecture serves as a breast model which is modelled based on the real-life breast phantom. System Identification method in MATLAB is used to get the dynamic structures and characteristics of the phantom [13]. A F/T sensor is used to obtain the actual force, F_a when the end-effector of the robot made contact to the target environment. Thus, a dedicated force control law can then be developed with the actual contact force information so that the robot can successfully maintain low contact force during the breast biopsy procedure.

In developing the force controller and control system for the UGBB robotic system, each of the simulations is divided into three sections to better analyze the control performance and to realize the real-life breast biopsy procedures; pre-contact, during contact, and post-contact operation. In the pre-contact operation, initial desired contact force was set at 0 N so that the robot end-effector merely touches the surface of the breast model without exerting any forces and also serves as the base reference of the response. During the breast contact operation, desired contact force was set at a unity input of 1 N and half phase of the respiration disturbance is introduced. The post-contact operation simulates the condition when the biopsy procedure is complete and the robot end-effector moves back to the surface of the breast model.

II. CONVENTIONAL PID FORCE CONTROLLER

Applications based on control theory have gone through major expansions in the past decades. It is noted that more than half of the industrial controllers operational today are PID controllers or modified PID controllers [14]. One of the reasons being its general applicability to most control system. In particular, when the mathematical model of the plant is unknown, the performance requirements are modest and so analytical design approaches are irrelevant, PID controls prove to be most convenient. In the field of process control systems, it is well known that the basic and modified PID control schemes have proved their practicality in delivering reasonable control, even though in many given conditions they may not provide the finest control.

The PID controller, as the name suggest, fundamentally has three parameters namely proportional gain (K_p), integral gain (K_i), and derivative gain (K_d). PID controller has several important functions; it provides feedback, the integral action able to reject steady-state offsets, and the derivative action can anticipate the future [15]. Several benefits for choosing the controller are the simplicity of the control law and the fewer tuning parameters. Hence for these reasons, there are many different types of tuning rules available. Then again, finding the optimum parameters for the PID controller is a daunting task and in practice control engineers often use trial and error method for the tuning process [16].

Fig. 2 displays the force response of the proportional (P) force controller for variation of K_p values ranging from 0.5 to 2. Based on the result, in the event of pre-contact and post-contact operations, all of the responses are not able to reach the 0 N desired force. It can also be observed that the proportional gain has the influence of reducing the rise time but is not able to eliminate the disturbance error. In addition, even though the error seems to be reduced with increased proportional gain, increasing it too much higher than a value of $K_p \geq 2$ will lead to unwanted noise and extreme overshoot during the start of the simulation.

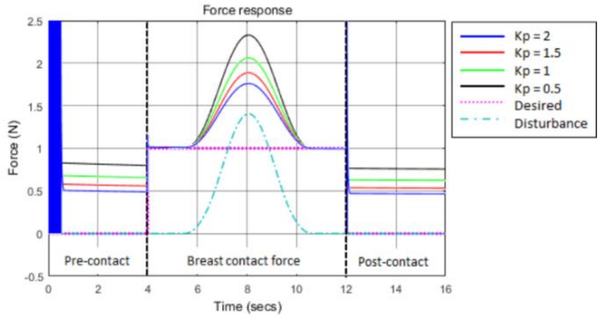

Figure 2: Force Response For Conventional Proportional Only PID Force Controller For Various *Kp* Gains

The force response of the proportional and integral (PI) force controller, for a variation of K_i gains is given in Fig. 3. The proportional gain was set at 1 while derivative gain was set at 0. It was later discovered that varying the derivative gain in this control system practically brings no effect at all, hence the reason on why PID controller is not developed. Based on the result, the integral term can be seen manage to accelerate the movement of the response towards desired set point, improve the transient response, and further reduces the disturbance error that occurs with a previously proportional only controller. However, while the error is reduced with increasing integral gain, the force response also introduces large overshoot during the start of the simulation. All things considered, getting the ideal gain parameters to achieve desired force response performance from a conventional PID force controller is time consuming and at the end comes at a cost of a large overshoot when the simulation started.

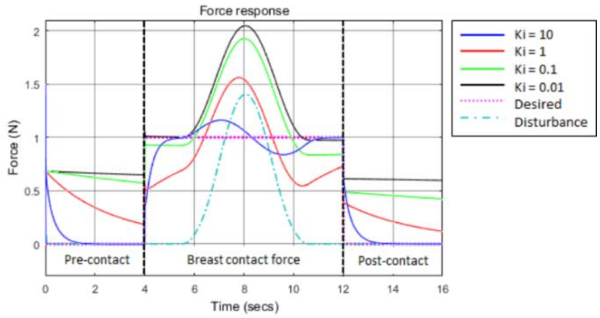

Figure 3: Force Response for Conventional PI Force Controller For Various K_i Gains

III. INTELLIGENT APPROACH TO THE FORCE CONTROLLER

Intelligent control techniques such as fuzzy logic control has the ability to include decision making and heuristics into the complex system controller design. In particular, fuzzy logic controller is advantageous for plants having inconveniences in deriving mathematical models or having performance limitations with conventional linear control schemes [17]. Considering that a nonlinear controller can control a nonlinear process more efficiently, fuzzy logic controller can also provide better performance in terms of rise time and smaller overshoot [18]. Based on discussions from previous results, conventional PID force controller cannot meet the control precision and requirements of the UGBB robotic system. Thus, the main objective in developing intelligent force controller is so that the resulting force controller response successfully meets the desired control performance.

A. PI-Fuzzy Force Controller

The advantage of using PI-Fuzzy controller over a conventional PI controller is that nonlinear control strategies can be implemented since it uses linguistic rules for the fuzzy component. Nevertheless, the most difficult problem and time consuming with this method is the parameter tuning, especially considering that the fuzzy logic has higher resolution of membership rules. The objective of the tuning is to select the suitable combination of PI gain and fuzzy logic parameters so that the resulting force controller response meets the desired control performance.

The proposed PI-Fuzzy controller has the gain of K_p and K_i set at 3 and 2 respectively. The matrix representation of the fuzzy rules is given in Table 1. From the table, row captions in the matrix contain the values for the actual force error signal as the first input, column captions contain the values for the change of error as the second input, and each cell is the resulting command when the input variables take the values in that row and column. The PI-Fuzzy force controller input variables are normalized into seven linguistic labels; negative big (NB), negative medium (NM), negative small (NS), zero (Z), positive small (PS), positive medium (PM) and positive big (PB).

Table 1
PI-Fuzzy Force Controller Membership Functions

	Error						
ΔError	NB	NM	NS	Z	PS	PM	PB
NB	NB	NB	NM	NM	NS	NS	Z
NM	NB	NM	NM	NS	NS	Z	PS
NS	NM	NM	NS	NS	Z	PS	PS
Z	NM	NS	NS	Z	PS	PS	PM
PS	NS	NS	Z	PS	PS	PM	PM
PM	NS	Z	PS	PS	PM	PM	PB
PB	Z	PS	PS	PM	PM	PB	PB

The characteristic surface between fuzzy inference system (FIS) inputs (force error, E and change of force error, CE) and FIS output (the desired incremental of robot position) is depicted in Fig. 4. Here, the tasks of fuzzification, Mamdani-type inference, and centroid defuzzification have been performed for all possible combinations of the inputs in the universe of discourse. The control surface plot presents the nonlinearity of the PI-Fuzzy controller as an effective force control method; the output incremental is gradual for all possible conditions.

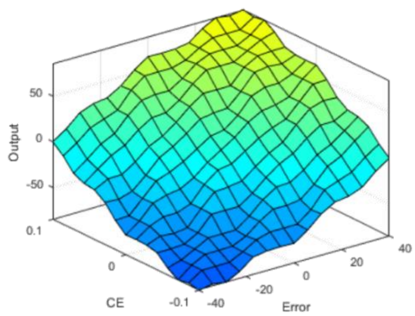

Figure 4: Control Surface of PI-Fuzzy Force Controller

The result for the force response of this type of controller to the overall UGBB robotic system is given in Fig. 5. The system has desired initial robot position set at 300 mm (contact point of the breast) and a unit step input of 1 N with a step time of 2 s. The response is slow with a rise time of about 1.6 s while the actual force is 0.9980 N (0.2% error) when there is no disturbance and topping at 1.0105 N (1.05% error) during the disturbance. It was observed that larger proportional gain will slightly increase the rise time but at the expense of higher steady-state error especially during the respiration disturbance. Increasing the integral gain would affect in extended rise time too but with a marginally reduced steady-state error.

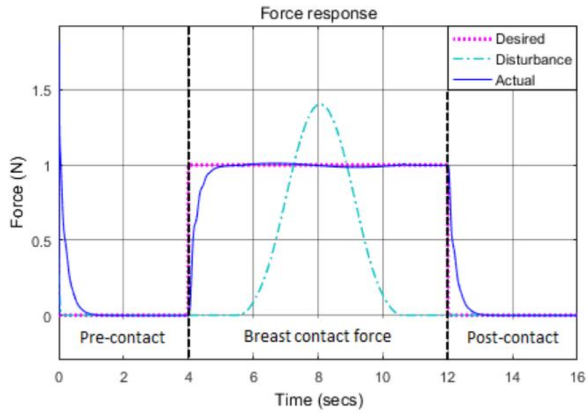

Figure 5: Force Response for PI-Fuzzy Force Controller

B. Fuzzy-PID Force Controller

The same structure of FIS two-input one-output is used based on the PI-Fuzzy force controller developed in earlier section. The PID gains of K_p, K_i and K_d are set at 0.5, 500 and 0.001 based on the knowledge from previous PID force controller. However, the change of measurement, *y(k)-y(k-1)* is used instead of change of error, *e(k)-e(k-1)* as the second input signal to the FIS in order to avoid the step change on reference signal from directly triggering the derivative action. To reduce complication in developing the fuzzy rules structure, minimal membership function is used to the point that only three linguistic variables are introduced; negative (N), zero (Z), and positive (P).

The generated nonlinear control surface as shown in Fig. 6 has higher gain near the center of the error and change of error if compared with a similar but linear control surface. This feature contributes to rapid error minimization whenever the error is small. On the other hand, the controller becomes less aggressive when the error is large so that control action is limited to avoid possible saturation. Smooth transitions across switching curves makes the F-PID force controller more robust to parameter variations [19].

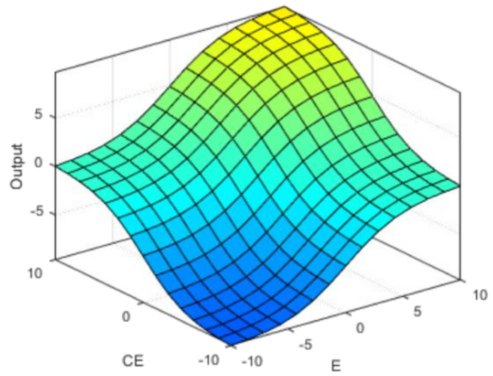

Figure 6: Control Surface for Fuzzy-PID Force Controller

As a result, the force response of this controller is presented in Fig. 7 with a rise time faster than that of the PI-Fuzzy force controller at about 11.2 ms. However, the F-PID force controller build up a slight overshoot of 1.31% for the same 1 N desired contact force. Further on the bright side, the actual force is recorded accurately at 1 N when there is no disturbance with a maximum error of just 0.0033 N or 0.33% during the respiration disturbance. Additionally, it can also be seen that unlike previous force controllers, the F-PID force controller does not developed any noticeable errors during the pre-contact and post-contact operations. This simulation result proves that with combined force and position control, the developed UGBB robotic system is able to effectively maintain desired contact force not just during the breast biopsy session (regardless of the respiration disturbance) but also throughout both before and after operations.

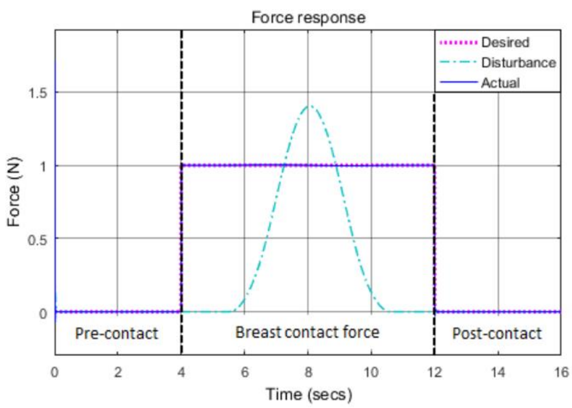

Figure 7: Force Response for Fuzzy-PID Force Controller

C. *Fuzzy-PID Force Controller using Lookup Table*

By replacing a Fuzzy Logic Controller block in former section with a Lookup Table block in Simulink, a fuzzy controller can be deployed with even simplified generated code and improved execution speed [20]. The motivation to advance with Fuzzy-PID controller using Lookup Table (F-LUT) is because the control scheme can provide a much broader range of break points to obtain sufficient approximation without the hassle of developing complicated Fuzzy membership function. These multiple break points are achievable since it possessed a smooth transition of nonlinear control surface as previously shown in Fig. 6. Another reason is to see whether it can deliver a better control performance than the F-PID controller.

The outcome of this force controller is shown in Fig. 8. At a rise time of 10.95 ms, it is a nominal improvement by 2.23% on initial speed response when compared to the same control structure but without using the Lookup Table. The actual force on the other hand has about the same performance but is marginally lower; 0.34% error when there is a disturbance and no error when the disturbance is absent. Besides, the overshoot is slightly higher at 1.48% compared to the F-PID force controller. Since the objective of the research is to maintain low contact force of the UGBB robotic system on the breast, thus F-PID force controller is chosen since the error is slightly lower with less overshoot than the rest of the established force controllers.

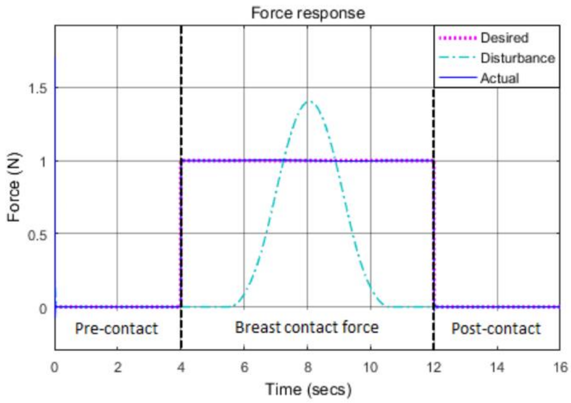

Figure 8: Force Response for F-LUT Force Controller

IV. Comparison of Force and Position Responses on Different Environment Conditions

In this section, simulation comparisons between position controller with selected F-PID force controller on separate environment conditions are validated. Simulations for all conditions were executed with the following constant variables:

1. Initial condition of the robot end-effector at 782 mm from the base point (robot at home position).
2. Contact point of the breast model, X_c at 300 mm from the base of the robot.
3. Initial desired position, X_d of the robot end-effector at 1 mm below the contact point of the breast model.
4. Desired force of F_d = 2N during the breast contact operation.
5. Introduction of respiration disturbance from 5.55 s until 10.55s.
6. Extreme disturbance of force unit up to 34.05N is considered in the last section of the simulations.

A. *Position Control System without Force Controller*

In this simulation, the force controller is disabled so that the system only functions with position controller of the RV-2AJ robot itself. Meanwhile, the force sensor is still active in order to monitor the exerted force from the robot end-effector towards the breast model.

From Figure 9, the actual force is nearly constant throughout the simulation apart from the disturbance period. However, since the simulation was conducted with only position controller without any form of feedback from the actual force to the entire system, the desired force of F_d = 2

N is nowhere achievable. Similarly, there is no deviation on robot position to compensate for the force error when the respiration disturbance is introduced. In this case, the robot position controller did not react accordingly and simply neglects the disturbance.

On the contrary, despite the total failure of the system at gaining the desired contact force, the robot is still able to successfully attain its initially desired position of X_d = 299 mm. This is due to the high accuracy of the developed robot's position controller with forward and inverse kinematics' accuracy at 98.68% and 97.72% up to 99.83% respectively as examined in Chapter 4. As a result, the actual force exerted by the robot arm at 1 mm below the contact point of the breast model remained at around 1 N without any noticeable changes. Unfortunately, due to the lack of additional force control, high force of about 2.8 N is applied towards the breast when the respiration disturbance is presented.

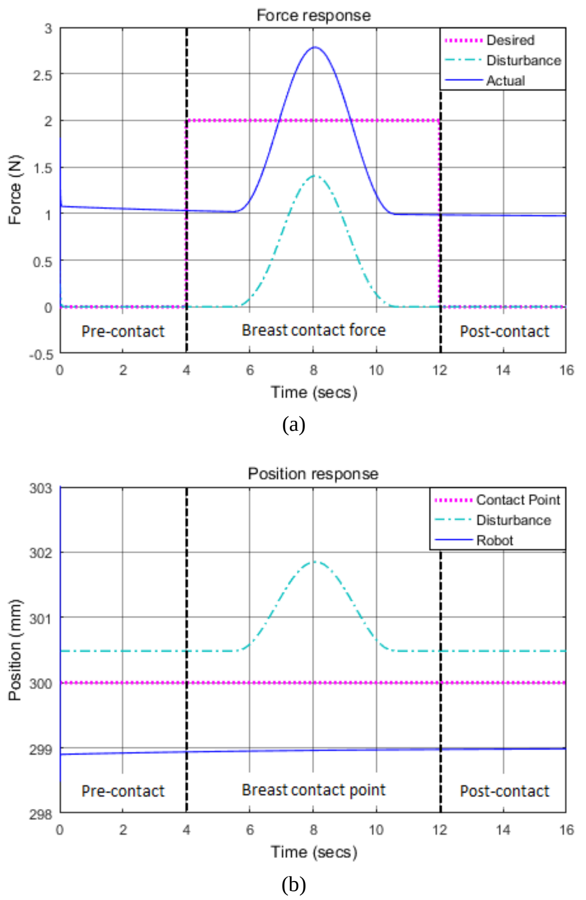

Figure 9: (a) Force and (b) Position Response of Position Control System Without Force Controller

B. Force/Position Control System with Breast Phantom as Environment (without Respiration Disturbance)

During the simulation in this section, both position and force controllers are operational but with only breast phantom served as the environment. External disturbance from the respiration is disabled. As such, the output response from position and force control is presented in Fig. 10. Since there is no respiration disturbance involved, the force and position response can be effectively held steady without error throughout the simulation in all kinds of contact operation. From the figures, the actual force can be seen remained at the desired target while the end-effector of the robot successfully maintains its corresponding position.

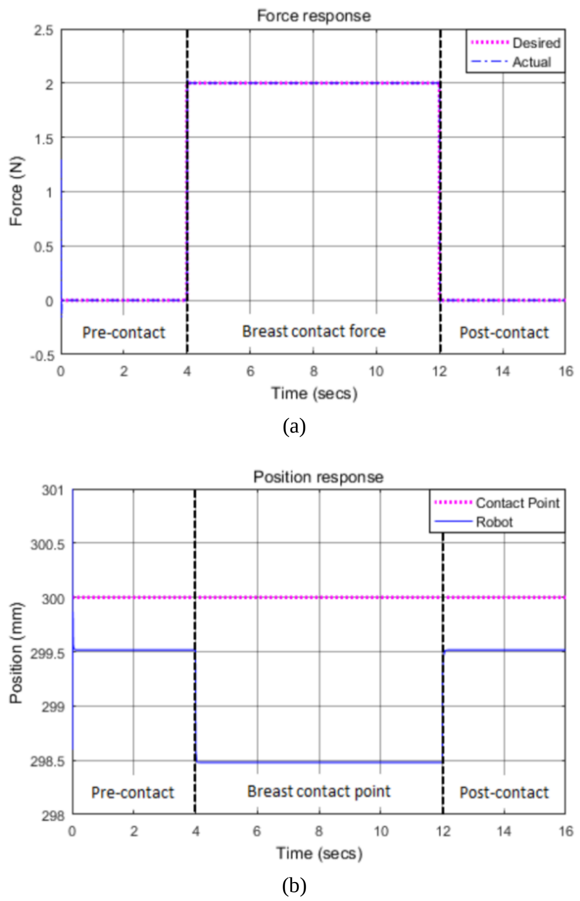

Figure 10: (a) Force and (b) Position Response for Position And Force Control System With Breast Phantom As Environment (Without Respiration Disturbance)

C. Force/Position Control System with Respiration Disturbance Effect

In this section, respiration disturbance is considered as the external factor that can caused instability to the system. Both force and position response are provided in Fig. 11. Based on these results, it is observable that the actual force, F_a successfully follows the desired force, F_d throughout all contact operations. Even when the respiration disturbance is introduced during the 5.55 – 10.55 s period, there is no noticeable errors for the actual force. In fact, the force error due to the disturbance only deviates by about ±0.0033 N. This proves that the developed force controller is essential in UGBB robotic system to maintain the desired contact force and to reject possible disturbance. Additionally, the robot position can be seen compensating for the disturbance by closely following the movement of the respiration. The difference in peak amplitude of the robot position compared with the peak amplitude of the respiration is only 0.0001 mm with the robot reaction slightly lagging by 1.7ms.

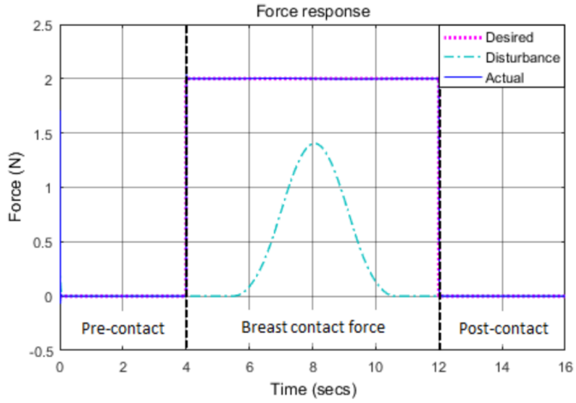

(a)

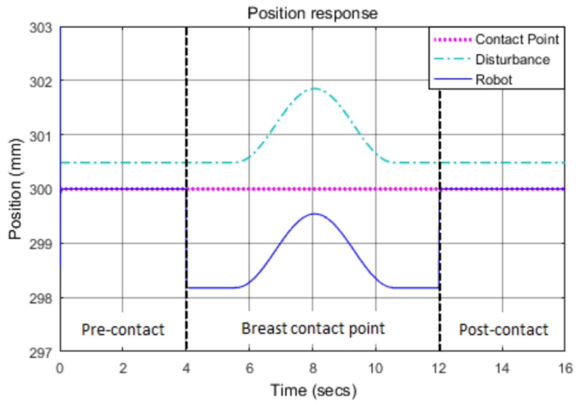

(b)

Figure 11: (a) Force and (b) Position Response for Position And Force Control System With Breast Phantom And Respiration Disturbance As Environment

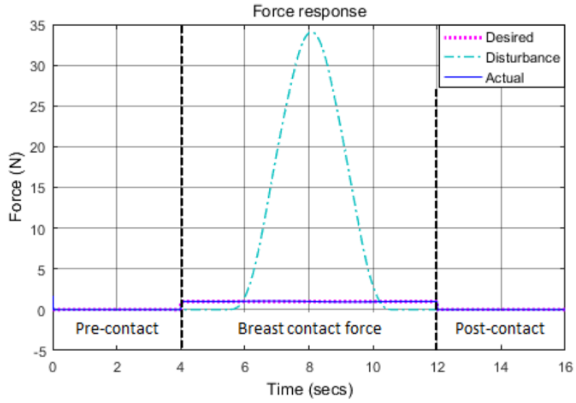

(a)

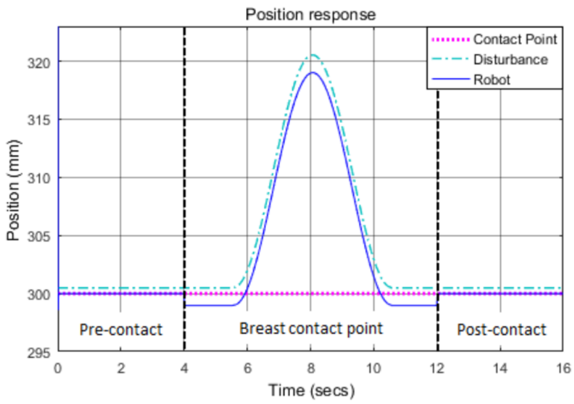

(b)

Figure 12: (a) Force and (b) Position Response for Position And Force Control System With Breast Phantom And Extreme Disturbance As Environment

D. Force/Position Control System with Extreme Disturbance

In certain cases, extreme disturbance is considered if there is a large force disturbance being acted towards the robot end-effector, for example the possibility of the patient's movement towards the robot while the biopsy operation is conducted. Based on the responses of both force and position presented in Fig. 12, the disturbance was designed so that it has about 20 mm of peak movement in *z* axis with 34.05 N of force. During this extreme disturbance period, the maximum error from the actual force was recorded at only ±0.05 N deviations from the desired contact force of 2 N, which brings it to just 2.5% error.

Subsequently, the efficiency of the developed force and position controllers made the robot position to follow along the trajectory of the disturbance with a steady-state error of only 0.0002 mm. In a nutshell, even with a very large force disturbance, the UGBB robotic system can still maintain its desired contact force without any noticeable and significant errors. This simulation further proves the effectiveness of the developed hybrid force and position controller for the UGBB robotic system.

V. Conclusion

Different set of force controllers have been established for the development of UGBB robotic system. Thorough analysis has been presented with the F-PID force controller having the most desirable performance with no error when the disturbance is lacking, the lowest error at 0.33% when the disturbance is present, and marginally low overshoot of 1.31%. Comparison of force and position responses on different environment conditions prove the viability of the force controller to be implemented on a real hardware setup. The simulation result also shows the efficiency of the force controller in successfully rejecting extreme disturbance of 34.05 N. Based on the results of the proposed UGBB robotic system, large deformations of the breast tissue could be reduced, and suspected lump can be effectively contained inside the ultrasound-imaging region by actively maintaining low contact force between the ultrasound probe and the patient's breast.

Acknowledgment

This work was supported by Ministry of Education and Universiti Tun Hussein Onn Malaysia under Research Acculturation Grant Scheme Vot R032.

References

[1] M. Clinic, "Breast biopsy - What you can expect," 2014. [Online]. Available: http://www.mayoclinic.org/tests-procedures/breast-biopsy/details/what-you-can-expect/rec-20236113. [Accessed: 14-Feb-2014].

[2] P. Britton *et al.*, "One-stop diagnostic breast clinics: how often are

breast cancers missed?," *Br. J. Cancer*, vol. 100, no. 12, pp. 1873–8, Jun. 2009.

[3] R. E. Fine and E. D. Staren, "Percutaneous radiofrequency-assisted excision of fibroadenomas," *Am. J. Surg.*, vol. 192, no. 4, pp. 545–547, 2006.

[4] L. K. Killebrew and R. H. Oneson, "Comparison of the diagnostic accuracy of a vacuum-assisted percutaneous intact specimen sampling device to a vacuum-assisted core needle sampling device for breast biopsy: Initial experience," *Breast J.*, vol. 12, no. 4, pp. 302–308, 2006.

[5] A. Koskela *et al.*, "Learning curve for add-on stereotactic core needle breast biopsy," *Acta radiol.*, vol. 47, no. 5, pp. 454–460, 2006.

[6] C. Zuiani, V. Londero, A. Bestagno, F. Puglisi, C. Di Loreto, and M. Bazzocchi, "Proliferative high-risk lesions of the breast: Contribution and limits of US-guided core biopsy," *Lesioni proliferative della mammella ad alto rischio Apporto e limiti della core biopsy*, vol. 110, no. 5–6, pp. 589–602, 2005.

[7] C. Salem, R. Sakr, J. Chopier, C. Marsault, S. Uzan, and E. Daraï, "Accuracy of stereotactic vacuum-assisted breast biopsy with a 10-gauge hand-held system," *The Breast*, vol. 18, no. 3, pp. 178–182, Jun. 2009.

[8] T. R. Nelson, A. Tran, H. Fakourfar, and J. Nebeker, "Positional Calibration of an Ultrasound Image-Guided Robotic Breast Biopsy System," *J. Ultrasound Med.*, vol. 31, no. 3, pp. 351–359, Mar. 2012.

[9] V. Mallapragada, N. Sarkar, and T. K. Podder, "Autonomous coordination of imaging and tumor manipulation for robot assisted breast biopsy," in *2008 2nd IEEE RAS & EMBS International Conference on Biomedical Robotics and Biomechatronics*, 2008, pp. 676–681.

[10] J. De Schutter and H. Van Brussel, "Compliant Robot Motion II. A Control Approach Based on External Control Loops," *Int. J. Rob. Res.*, vol. 7, no. 4, pp. 18–33, Aug. 1988.

[11] V. Perdereau and M. Drouin, "About kinematic local instability and stabilization of hybrid control schemes," in *Proc. of ISRAM '94*, 1994, pp. 545–530.

[12] A. Pujas, P. Dauchez, and F. Pierrot, "Hybrid position/force control: task description and control scheme determination for a real implementation," in *Proceedings of 1993 IEEE/RSJ International Conference on Intelligent Robots and Systems (IROS '93)*, 1993, vol. 2, no. C, pp. 841–846.

[13] M. A. Ayob, W. N. Wan Zakaria, J. Jalani, N. Mohamed Nasir, and M. R. Md Tomari, "Estimation of nonlinear ARX model for soft tissue by wavenet and sigmoid estimators," *J. Telecommun. Electron. Comput. Eng.*, vol. 8, no. 7, pp. 123–128, Apr. 2016.

[14] K. Ogata, *Modern control engineering*, 5th ed. Pearson, 2009.

[15] K. Astrom, *PID controllers: theory, design and tuning*. ISA: The Instrumentation, Systems, and Automation Society, 1995.

[16] Emerson, "PID tuning," 2016. [Online]. Available: https://www.automationworld.com/lean-manufacturing/pid-tuning. [Accessed: 15-Dec-2016].

[17] D. Fuyin and D. Weifeng, "Design of a three-input fuzzy logic controller and the method of its rules reduction," in *Proceedings of the 2009 International Symposium on Information Processing (ISIP'09)*, 2009, vol. 2, pp. 51–53.

[18] A. A. Khan and N. Rapal, "Fuzzy PID Controller: Design, Tuning and Comparison with Conventional PID Controller," in *2006 IEEE International Conference on Engineering of Intelligent Systems*, 2006, no. 1, pp. 1–6.

[19] A. Kandel and G. Langholz, *Fuzzy Control Systems*, 1st ed. CRC Press, 1993.

[20] Mathworks, "Using Lookup Table in Simulink to Implement Fuzzy PID Controller," 2017. [Online]. Available: http://www.mathworks.com/help/fuzzy/examples/using-lookup-table-in-simulink-to-implement-fuzzy-pid-controller.html?prodcode=FL&language=en. [Accessed: 17-Feb-2017].